Research Article Vol. 30, No. 10 / 9 May 2022 / Optics Express 17164
Optics EXPRESS

Distributed measurement of mode group effective refractive index difference in a few mode optical fibers

KRZYSZTOF MARKIEWICZ,[1,2,*] ŁUKASZ SZOSTKIEWICZ,[2,3] JAKUB KACZOROWSKI,[1,2] ZHISHENG YANG,[1,4] ALEJANDRO DOMINGUEZ-LOPEZ,[2] MAREK NAPIERAŁA,[2] TOMASZ NASIŁOWSKI,[2] AND LUC THÉVENAZ[1]

[1]*EPFL Swiss Federal Institute of Technology, Group for Fibre Optics, SCI STI LT, Station 11, 1015 Lausanne, Switzerland*
[2]*InPhoTech Sp. z o. o., Poznanska 400, Oltarzew, 05-850, Poland*
[3]*Faculty of Physics, Warsaw University of Technology, ul. Koszykowa 75, 00-662 Warsaw, Poland*
[4]*Present address: State Key Laboratory of Information Photonics & Optical Communications, Beijing University of Posts and Telecommunications, Beijing 100876, China*
[*]*kmarkiewicz@inphotech.pl*

Abstract: The possibility to perform distributed measurements of the effective refractive index difference between distinct modes in few mode optical fibers is demonstrated using phase sensitive optical time domain reflectometry. Effective refractive index differences between LP02, LP21a and LP21b modes are measured with for a spatial resolution of 24m.

1. Introduction

Optical time domain reflectometry (OTDR) is the most common inspection technique used to detect failures in deployed optical fiber networks. Researchers who proposed OTDR for the first time recognized the potential of the technique, but its importance in sustaining passive optical networks was hard to predict back in the 70s [1]. OTDR measurement provides information about spatially resolved optical attenuation which allows events such as fiber breakage, bad splicing, connectors, or splitters to be identified. OTDR is relatively insensitive to more subtle disturbances such as temperature/strain variations or fiber birefringence. To measure these quantities, coherent optical time domain reflectometry (C-OTDR) was proposed [2]. This technique, in comparison to classical OTDR, uses a coherent, tunable light source and measures similarity [3] between the fiber time domain response, called a trace, before and after the induced change. Moreover, it is possible to modify the original C-OTDR setup to measure, for example, the birefringence of birefringent optical fibers [4], optical fiber shape using multicore fibers [5,6], detect seismic waves [7] or perform measurements on multimode fibers [8]. The examples presented, represent only a few amongst many permutations of C-OTDR based sensing techniques [9,10] that can be utilized with new, potential applications that are still arising.

One of the properties of optical fibers that had thus far remained unmeasured in a distributed manner was the intermodal effective refractive index difference in multimode and few mode fibers. The major difference between distributed birefringence measurements and intermodal measurements is the mode spatial distribution that is almost identical in the case of single mode birefringent fibers. In the case of a single mode optical fiber, one can expect that the wavelength shifted C-OTDR wavelength scan will produce identical trace spectra due to the same distribution of scattering points interacting with the incident wave. In the few mode fiber case, the mode spatial distribution varies from mode to mode which means that the light effectively "sees" the different scattering centers and the traditional one dimensional model [11] of scattering centers

#455782 https://doi.org/10.1364/OE.455782
Journal © 2022 Received 9 Feb 2022; revised 15 Apr 2022; accepted 22 Apr 2022; published 3 May 2022

Optics EXPRESS

is no longer valid. The scattering centres are physically positioned identically for all modes, but their relative contribution for the light propagating in distinct modes is clearly different. The phase cumulated by the light backscattered from 2 given scattering centres will depend on the effective indices of the incident and collecting modes. As a result, the correlation of signals originating from spatially different modes will no longer produce straightforwardly comparable traces and therefore statistical analysis is required. In this paper, we show that even though the scattering characteristics of different modes are not identical after a laser frequency change, the statistical average of the maximum cross correlation values is matched with differences in the effective refractive indices of the modes.

Since few mode fibers [12,13] are one of the most promising transmission media that may allow the world capacity record to be broken [14], it can be predicted, with a reasonable degree of certainty, that they will be deployed on the field. This means that potential tools for an in depth characterization of this new type of fiber may prove useful - for example, for the precise spatially resolved differential group delay (DGD) measurements, that are potentially needed to provide the level of complexity required for Multiple Input Multiple Output algorithms [15], or for reducing the cross sensitivity of optical fiber sensors due to the potential accessibility of many independently changing variables under external perturbation. Proposed technique is applicable for measurements of effective refractive indexes but is not capable of performing absolute values measurement which is an inherent property of wavelength scanned C-OTDR system.

2. Theoretical prediction

In order to predict the expected frequency shifts needed to cross correlate traces from different groups present in the examined fiber, we have built a fiber numerical model with refractive index distribution presented in Fig. 1

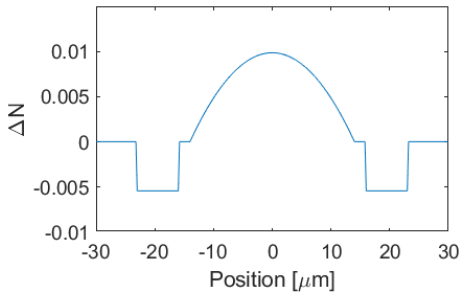

Fig. 1. Refractive index distribution of investigated few mode fiber

The fiber model is based on the finite-element method and assumes a 25 μm core diameter with a maximum refractive index difference of $\Delta n = 0.01$ for a 1550 nm wavelength with a parabolic refractive index distribution. The core is surrounded by a trench of Δn=−0.005 with a width of 6 μm. The distance between the core and the trench area is equal to 1.5 μm. The refractive indices of the points in the fiber core are calculated using the Sellmeier equations and take into account the chromatic dispersion [16]. The resulting effective refractive indices differences are used to calculate the theoretical frequency shift Δf needed to correlate the mode pairs. We can expect C-OTDR trace matching when following equation is satisfied:

$$n_{LPn1}(\lambda_1) * \lambda_1 = n_{LPn2}(\lambda_2) * \lambda_2, \tag{1}$$

where n_{LPn1} is effective refractive index for first mode at wavelength equal to λ_1, n_{LPn2} is effective refractive index for second mode at wavelength λ_2. In our calculations we assume that λ_1 is equal

Optics EXPRESS

to 1550 nm. To calculate spectral shift Δf following equation is used:

$$\Delta f = c\left(\frac{1}{\lambda_1} - \frac{1}{\lambda_2}\right), \tag{2}$$

where c stands for speed of light in vacuum. The results are presented in Table 1, where one can see that in most cases it is necessary to perform a scan over 200 GHz, which is beyond the measurement capability of classical C-OTDR interrogation setup. Mode pairs with expected frequency shift larger than 200 GHz are excluded from further analysis. We also excluded LP_{12}/LP_{31} mode pair due to practical limitations of mode multiplexer. The mode pair LP_{02}/LP_{21} was chosen for further analysis due the a small frequency shift (0.75 GHz) needed to correlate the signals. All mode pairs examined experimentally for frequency shifts are bolded in Table 1. The difference between LP_{21a} and LP_{21b} is equal to 0 which translates to a 0 GHz frequency shift. The zero difference between LP_{21a} and LP_{21b} is a result of having the same spatial distribution but rotated by 45 degrees. There is a difference between the theoretical frequency shift between the same pair of modes but in a different order, for example, the frequency shifts needed to correlate the LP_{13}/LP_{12} mode pair are 801.51 GHz and - 808.21 GHz depending on the reference mode. Asymmetry between result for the same pair of modes but in different order is a result of hyperbolic relation between difference of effective refractive indexes and λ_2 and due to the chromatic dispersion. The non-symetricity of values in Table 1 is increasing with the effective refractive index difference between the modes.

Table 1. Theoretical C-OTDR frequency shifts between mode groups in examined few mode fiber bolded numbers indicate mode pairs that are a subject of further analysis. Reference mode is given in column and is assumed to be measured at 1550 nm.

Δf [GHz]	LP_{01}	LP_{11}	LP_{21}	LP_{02}	LP_{31}	LP_{12}
LP_{01}	0.00	−269.10	−538.30	−539.06	−805.88	−808.21
LP_{11}	268.35	0.00	−268.45	−269.20	−535.29	−537.61
LP_{21}	535.32	267.70	0.00	**−0.75**	−266.10	−268.41
LP_{02}	536.07	268.46	**0.75**	**0.00**	−265.34	−267.66
LP_{31}	799.22	532.34	265.37	264.62	0.00	−2.31
LP_{12}	801.51	534.63	267.67	266.92	2.31	0.00

3. Experimental setup

The scheme of the setup is shown in Fig. 2(a)) [17]. A DFB laser operating at a central wavelength of 1550 nm is used as a light source. By changing the operating current of the laser, we tune the central frequency up to 20 GHz in steps of 75 MHz. Using a pulse generator, a 4 ns optical pulse is generated with an extinction ratio of more than 50 dB, which is more than sufficient for measurements of 1 km of fiber and corresponds to a 40 cm spatial resolution of the system. To increase the pulse power, an erbium doped fiber amplifier (EDFA) is inserted. Then the pulse goes through a mode multiplexer, which enables a single mode to be selectively excited in a few-mode fiber with a selectivity better than 15 dB and an average insertion loss of 3.5 dB. The generated pulse is sent in the LP_{01} mode of the fiber under test (FUT). The examined fiber is a 1 km long few-mode-fiber with cross section presented in Fig. 1. At each point of the FUT, the propagating pulse is partially scattered into all modes that are guided by the fiber and propagates backwards [18]). The FUT is stabilized in a water bath to reduce the influence of environmental perturbations such as vibrations or random temperature changes. By using a pair of optical switches, it is possible to select a signal backscattered into chosen higher order modes. In this experiment, modes LP_{21a}, LP_{21b}, LP_{02} have been measured because, according to Table 1,

Optics EXPRESS

the expected frequency shifts from these modes can be potentially measured using a 20 GHz frequency scan range. The spatial distributions of all the measured modes for a particular fiber are presented in Fig. 2(b), (c), (d) respectively. The returning signal is then amplified by a second EDFA. After the amplifier, a tunable filter with a bandwidth of 1 nm is used to filter out the amplified spontaneous emission. The filtered signal is measured by a DC-coupled photodetector with a 1 GHz bandwidth and digitized by a 4 GHz bandwidth oscilloscope with a sampling rate of 5 GSamples/s.

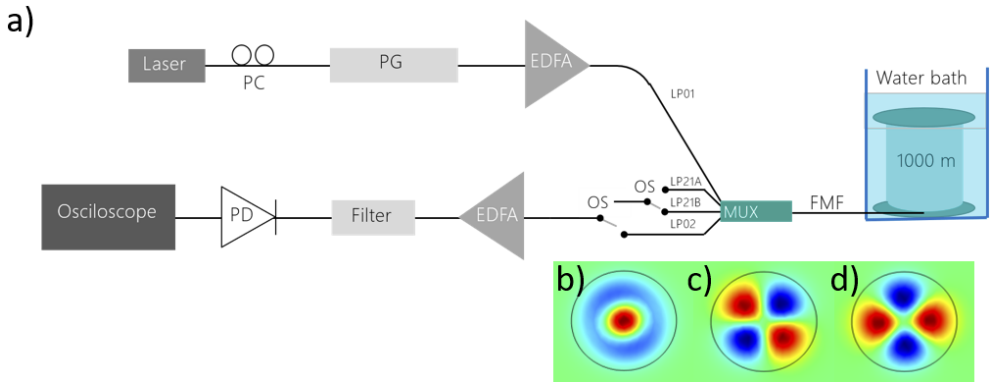

Fig. 2. Experimental setup. PC - polarization controller, PG – optical pulse generator, EDFA – erbium doped fiber amplifier, MUX – Mode Multiplexer, FMF – few-mode fiber, OS-optical switch, PD – photodiode. Spatial distribution of b) LP02, c) LP21a, d) LP21b

To verify the performance of the assembled setup we calculated the visibility of the obtained time domain trace according to the following formula:

$$Visibility = \frac{I_{max} - I_{min}}{I_{max} + I_{min}} \tag{3}$$

where I_{max} and I_{min} are respectively the maximum and the minimum intensity of the trace [19]. The visibility is calculated using a 40 m calculation window which corresponds to 100 spatial resolutions. The sample data obtained from acquiring a backscattered signal for LP_{02}, LP_{21a} and LP_{21b} from one pulse launched into mode LP_{01} is presented in Fig. 3. Measured traces are quasi random in nature and there is no simple similarity between them even though they originate from the same pump pulse with exactly the same wavelength. This proves that each trace has its origin from differently distributed scattering centers in an optical fiber. Such behavior is expected due to a different spatial overlap of incident light field and distribution of scattering points in cross section of any arbitrary fiber. In all cases the visibility is above 0.9 which means that the measurement system is working properly and information contained in the C-OTDR trace can be used for wavelength scanning C-OTDR [20]. Only at the beginning of the fiber the visibility is lower due to a strong reflection from the mode multiplexer.

Optics EXPRESS

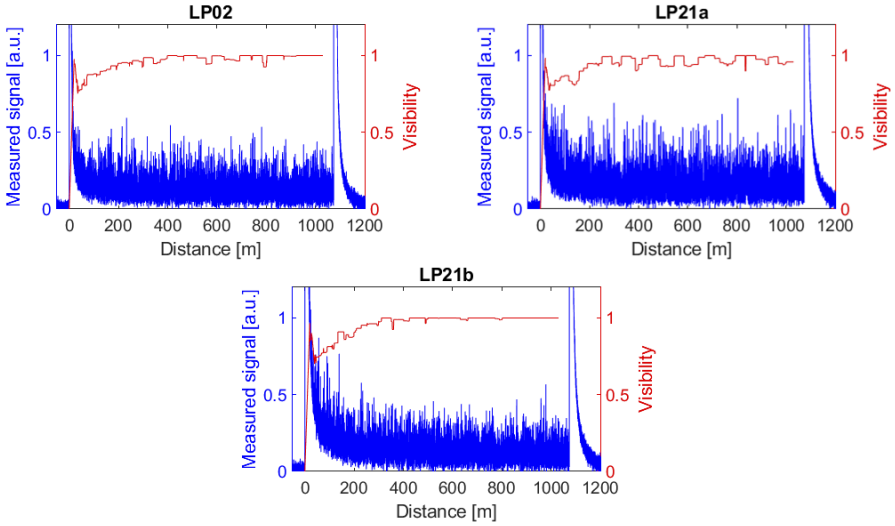

Fig. 3. Example of the measured time trace for LP02, LP21a and LP21b modes under LP01 excitation (blue line) and the calculated visibility of the traces (red line).

4. Results

To obtain the difference in effective refractive index between the measured higher order modes, the cross-correlation spectrum at every sampling point along the fiber is calculated. The cross correlation between two frequency scans for a signal scattered to the same mode LP_{02}-LP_{02} results in a clearly visible maximum at a 0 GHz frequency shift, which can be seen in Fig. 4(a)). When performing the same operation on signals originating from different modes, one can observe at first glance, quasi random cross correlation values with a maximum centered at 0 GHz due to the cross-correlation window envelope. The quasi-random cross-correlation spectra for LP_{21b}-LP_{02}, LP_{21a}-LP_{02} and LP_{21a}-LP_{21b} are presented on Fig. 4(b)), Fig. 4(c)) and Fig. 4(d)) respectively. Second given mode is a reference. Observed randomness of cross-correlation spectra is caused by the fact that each mode has substantially different spatial distribution and thus interacts with different scattering points distribution perpendicular to the light propagation direction. In the case of few mode fiber, one can't expect perfect trace matching because only a fraction of refractive index fluctuations (parallel to the propagation direction) are common for all modes. This is a major difference comparing to single mode C-OTDR scenario when fluctuations of refractive index perpendicular to the light propagation does not play a role Performing further analysis of the intermodal cross-correlation spectra, we define the coefficient κ as the average of the cross-correlation value which can be expressed by equation:

$$\kappa(\Delta f) = \sum_{n=L1}^{L2} \frac{I_n(\Delta f)}{L1 - L2} \tag{4}$$

where $L1$ and $L2$ represents location of extreme points for κ calculation and I_n is a cross correlation amplitude measured at frequency shift Δf. For initial analysis we consider $L1 = 0$ and $L2 = 1000\ m$ which is entire fiber span and plot κ against the laser spectral shift in Fig. 5. As expected, the maximum of κ for LP_{02}-LP_{02} is positioned close to 0 GHz at 0.06 GHz which can be attributed to temperature variations occurring during the experiment (which, in this case, did not exceeding 0.3 K). In the case of the $LP_{21a,b}$-LP_{02} mode pairs it can be noticed that the maximum value of κ is shifted accordingly to the Table 1, and is equal to 0.83 GHz and 0.89 GHz for LP_{21a}-LP_{02} and LP_{21b}-LP_{02} respectively. The difference of 19% between expected and measured

Optics EXPRESS

value can be associated with the fact that the comparison is made between numerical model and demonstrated measurement. In that case, true value of effective refractive index difference between modes is not known. The decreased maximum value of κ can be associated with a substantially different spatial distribution of mode profiles resulting in different spatial overlaps with scattering centers in the examined fiber.

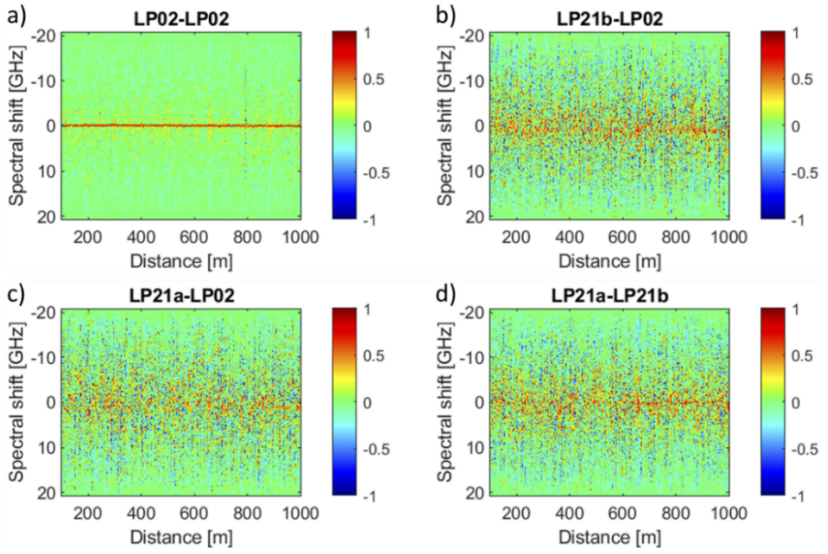

Fig. 4. Cross correlation values as a function of spectral shift and fiber distance for a) LP02-LP02 b) LP21b-LP02, c) LP21a-LP02 and d) LP21a-LP21b mode pairs. Second given mode is a reference.

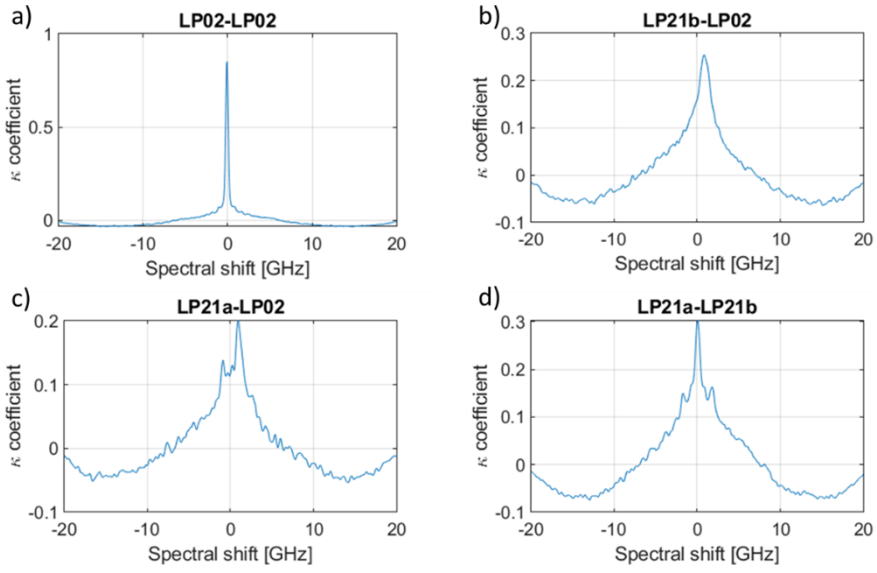

Fig. 5. Average normalized cross correlation value over entire fiber span for for a) LP02-LP02 b) LP21b-LP02, c) LP21a-LP02 and d) LP21a-LP21b mode pairs. Second given mode is a reference.

Optics EXPRESS

A comparison of theoretical values with experimental ones is presented in Table 2. The 0.06 GHz frequency shift present for LP_{02} - LP_{02} and LP_{21a}-LP_{21b} can be associated with slight (<0.3 K) temperature variations between consecutive measurements. The measured spectral shift between LP21b-LP02 and LP_{21a}-LP_{02} is in line with the expectations presented in Table 1. Table 2 also presents calculated difference in effective refractive index (Δneff) and DGD as an example of useful output information resulting from proposed technique.

Table 2. Comparison of experimental and theoretical frequency shifts needed to correlate backscattered signals from different modes

Δf [GHz]	Theoretical	Experimental	Δneff (10^{-6})	DGD (ps/km)
LP_{02} - LP_{02}	0	-0.064 ± 0.003	0.48 ± 0.02	1.62 ± 0.07
LP_{21b}-LP_{02}	0.75	0.835 ± 0.036	6.33 ± 0.27	21.11 ± 0.91
LP_{21a}-LP_{02}	0.75	0.899 ± 0.047	6.81 ± 0.36	22.73 ± 1.19
LP_{21a}-LP_{21b}	0	0.064 ± 0.041	0.48 ± 0.31	1.61 ± 1.04

In this particular case (Fig. 5 and Table 2) we used the whole fiber length for the calculation of κ; however, it is possible to choose any arbitrary calculation window to resolve the distributed information about the intermodal effective refractive index difference and the corresponding frequency shift variations. Decreased spatial window for calculation of κ results in an increased standard deviation. The relation between the number of spatial resolutions taken for the calculation of κ and the calculated spectral shift is presented in Fig. 6. The error bars indicate one standard deviation of κ.

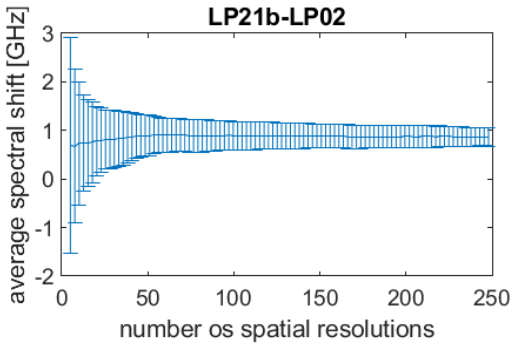

Fig. 6. Average spectral shift calculated using κ parameter as a function of spatial resolutions used for calculations. Error bars indicate standard deviation for κ. LP21b is a reference mode.

According to Fig. 6, one can conclude that the standard deviation of κ decreases rapidly with the number of spatial resolutions up to the value of 60 spatial resolutions. Rapid decrease of standard deviation with a number of samples taken into calculation is typical statistical property and can be explained by Central Limit Theorem. Therefore, we chose 60 optical spatial resolutions as a calculation window. In this case, each point for cross correlation calculation has 40 cm of optical spatial resolution. As a result, the measurement demonstrated in Fig. 7 has 24 m spatial resolution ($L1 - L2 = 24$m according to Eq. (**2**)). Standard deviation for 24 m calculation window is 0.35 GHz. The results are presented in Fig. 7. Black line represents measured maximum value of κ.

A direct comparison of Fig. 4 and Fig. 7 shows that simple statistical analysis of intermodal cross correlation can result in a reliable measurement even though the traces are hardly comparable at first sight. Potential effects of intermodal crosstalk can be associated with occasionally

Optics EXPRESS

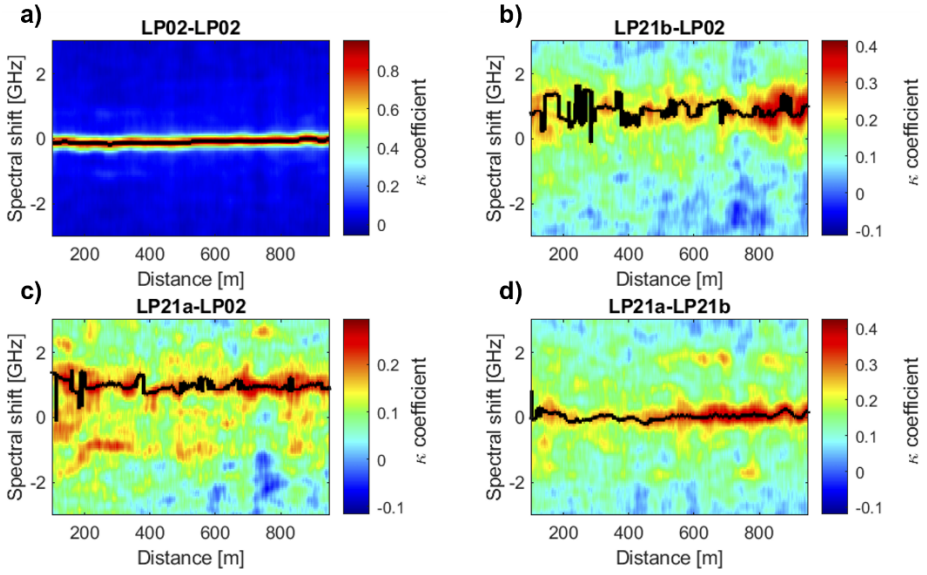

Fig. 7. Spatially resolved intermodal spectral shift calculated using κ and 60 spatial resolutions calculation window for a) LP02-LP02 b) LP21b-LP02, c) LP21a-LP02 and d) LP21a-LP21b mode pairs. Second given mode is a reference. Black line represents measured maximum value of κ.

measurable double maximum of κ especially visible in Fig. 7(c)) at the 200 m-300 m fiber section. Detailed difference between local cross correlation spectrum (blue line) and κ coefficient (black line) calculated at 812 m of the fiber is presented in Fig. 8. While the cross-correlation spectrum does not indicate any clear peak, the κ coefficient is clearly distinguishable. As the scattering points "seen" by different modes do not share the same distribution perpendicular to the light propagation and only the parallel distribution is common, the statistical approach is necessary to extract useful information.

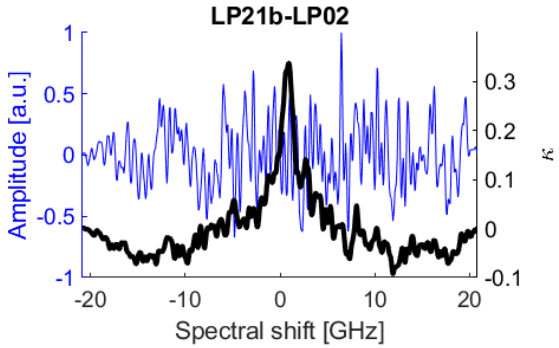

Fig. 8. Comparison between cross correlation spectrum (blue line) measured at 812 m and κ coefficient (black line) calculated from fiber segment starting at 800 m and finishing at 824 m

A downside of this statistical approach is reduction in the real spatial resolution of measurement. The exact relations between interrogating pulse width and necessary number of spatial resolutions that need to be averaged remains to be examined in the future.

Optics EXPRESS

5. Conclusion

We demonstrated that it is possible to measure the effective refractive index between modes in few mode optical fibers in a distributed manner. The measured spectral shift matches theoretical values and even though the modes have substantially different spatial distributions resulting in a reduced maximum cross correlation value, it is possible to statistically measure the spectral shift between the modes. The improvement of proposed technique, in terms of the number of modes that can be correlated, is potentially possible using larger scanning range of the laser source. Further study must follow to verify if it is possible to correlate very distinct modes in multimode fibers with reduced spatial overlap. One of the possible ways to corelate distinct modes is to use Optical Frequency Domain Reflectometry(OFDR) technique [21], which can offer tuning range in the order of tens of nanometers but with reduced sensing distance. Potentially, proposed technique opens a possibility to make tens of independent measurements from one fiber. Such feature may be used for multiparameter sensing using a few mode fiber as well as for in depth characterization of fiber uniformity.

Funding. Fundacja na rzecz Nauki Polskiej (NODUS, TEAMTECH); Narodowe Centrum Badań i Rozwoju (TECHMATSTRATEG1/348438/16/NCBR/2018).

Disclosures. The authors declare no conflicts of interest.

Data availability. Data underlying the results presented in this paper are not publicly available at this time but may be obtained from the authors upon reasonable request.

References

1. M. K. Barnoski, M. D. Rourke, S. M. Jensen, and R. T. Melville, "Optical time domain reflectometer," Appl. Opt. **16**(9), 2375–2379 (1977).
2. Y. Koyamada, M. Imahama, K. Kubota, and K. Hogari, "Fiber-optic distributed strain and temperature sensing with very high measurand resolution over long range using coherent OTDR," J. Lightwave Technol. **27**(9), 1142–1146 (2009).
3. L. Zhang, Z. Yang, N. Gorbatov, R. Davidi, M. Galal, L. Thévenaz, and M. Tur, "Distributed and dynamic strain sensing with high spatial resolution andlarge measurable strain range," Opt. Lett. **45**(18), 5020–5023 (2020).
4. M. A. Soto, X. Lu, H. F. Martins, M. Gonzalez-Herraez, and L. Thévenaz, "Distributed phase birefringence measurements based on polarization correlation in phase-sensitive optical time-domain reflectometers," Opt. Express **23**(19), 24923–24936 (2015).
5. I. Floris, J. M. Adam, P. A. Calderón, and S. Sales, "Fiber Optic Shape Sensors: A comprehensive review," Opt. Lasers Eng. **139**, 106508 (2021).
6. Ł. Szostkiewicz, M. A. Soto, Z. Yang, A. Dominguez-Lopez, I. Parola, K. Markiewicz, A. Pytel, A. Kołakowska, M. Napierała, T. Nasiłowski, and L. Thevenaz, "High-resolution distributed shape sensing using phase-sensitive optical time-domain reflectometry and multicore fibers," Opt. Express **27**(15), 20763 (2019).
7. M. R. Fernandez-Ruiz, H. F. Martins, E. Williams, C. Becerril, R. Magalhaes, L. D. Costa, S. Martin-Lopez, S. Jia, Z. Zhan, and M. Gonzalez-Herraez, "Seismic Monitoring with Distributed Acoustic Sensing from the Near-surface to the Deep Oceans," J. Lightwave Technol. 1 (2021).
8. K. Markiewicz, J. Kaczorowski, Z. Yang, L. Szostkiewicz, A. Dominguez-Lopez, K. Wilczynski, M. Napierala, T. Nasilowski, and L. Thévenaz, "Frequency scanned phase sensitive optical time-domain reflectometry interrogation in multimode optical fibers," APL Photonics **5**(3), 031302 (2020).
9. P. Lu, N. Lalam, M. Badar, B. Liu, B. Chorpening, M. Buric, and P. R. Ohodnicki, "Distributed optical fiber sensing: Review and perspective," Appl. Phys. Rev. **6**(4), 041302 (2019).
10. X. Lu, "Coherent Rayleigh time domain reflectometry novel applications for optical fibre sensing," ÉCOLE POLYTECHNIQUE FÉDÉRALE DE LAUSANNE (2016).
11. A. H. Hartog, *An Introduction to Distributed Optical Fibre Sensors* (Taylor & Francis Group, 2017).
12. A. Li, Y. Wang, Q. Hu, and W. Shieh, "Few-mode fiber based optical sensors," Opt. Express **23**(2), 1139–1150 (2015).
13. S. Berdagué and P. Facq, "Mode division multiplexing in optical fibers," Appl. Opt. **21**(11), 1950–1955 (1982).
14. B. J. Puttnam, R. S. Luís, G. Rademacher, Y. Awaji, and H. Furukawa, "319 Tb/s Transmission over 3001 km with S, C and L band signals over gt;120 nm bandwidth in 125 μm wide 4-core fiber," in *2021 Optical Fiber Communications Conference and Exhibition (OFC)* (2021), pp. 1–3.
15. S. Ohno, D. Iida, K. Toge, and T. Manabe, "High-resolution measurement of differential mode delay of few-mode fiber using phase reference technique for swept-frequency interferometry," Opt. Fiber Technol. **40**, 56–61 (2018).
16. O. V. Butov, K. M. Golant, A. L. Tomashuk, M. J. N. Van Stralen, and A. H. E. Breuls, "Refractive index dispersion of doped silica for fiber optics," Opt. Commun. **213**(4-6), 301–308 (2002).

Optics EXPRESS

17. K. Markiewicz, J. Kaczorowski, Z. Yang, L. Szostkiewicz, A. Dominguez-Lopez, M. Napierała, T. Nasiłowski, and L. Thévenaz, "Intermodal measurements in few-mode fibers with phase- sensitive OTDR," in *Optical Fiber Sensors Conference 2020 Special Edition* (Optical Society of America, 2020), p. T3.4.
18. Z. Wang, H. Wu, X. Hu, N. Zhao, Q. Mo, and G. Li, "Rayleigh scattering in few-mode optical fibers," Sci. Rep. **6**(1), 35844 (2016).
19. H. F. Martins, S. Martin-Lopez, P. Corredera, M. L. Filograno, O. Frazao, and M. Gonzalez-Herraez, "Coherent noise reduction in high visibility phase-sensitive optical time domain reflectometer for distributed sensing of ultrasonic waves," J. Lightwave Technol. **31**(23), 3631–3637 (2013).
20. X. Lu, M. A. Soto, L. Zhang, and L. Thévenaz, "Spectral Properties of the Signal in Phase-Sensitive Optical Time-Domain Reflectometry With Direct Detection," J. Lightwave Technol. **38**(6), 1513–1521 (2020).
21. C. Liang, Q. Bai, M. Yan, Y. Wang, H. Zhang, and B. Jin, "A Comprehensive Study of Optical Frequency Domain Reflectometry," IEEE Access **9**, 41647–41668 (2021).